PHYSICAL REVIEW E **76**, 050403(R) (2007)

State diagram for the electrostatic adsorption of charged colloids on confining walls: Simulation and theory

J. J. Liétor-Santos,[1,*] M. Chávez-Páez,[2] M. Márquez,[3] A. Fernández-Nieves,[1,*] and M. Medina-Noyola[2]
[1]*Group of Complex Fluids Physics, Department of Applied Physics, University of Almeria, Almeria 04120, Spain*
[2]*Instituto de Fisica "Manuel Sandoval Vallarta," Universidad Autonoma de San Luis Potosi, Alvaro Obregón 64, Zona Centro, 78000 San Luis Potosi, S.L.P., Mexico*
[3]*Harrington Department of Bioengineering, Arizona State University, Tempe, Arizona 85287, USA*
(Received 1 June 2007; published 28 November 2007)

We study the structure of charged colloidal suspensions under confinement and determine a state diagram for the occurrence of electrostatic adsorption onto the confining walls, an effect that results in the accumulation of particles on the bounding surfaces and that could be relevant in experiments. We use Monte Carlo simulations to quantify this structural transition and perform theoretical calculations based on integral equations. Overall, our results provide a guide for experimentalists dealing with charged colloidal systems to determine the relevance of this purely electrostatic effect.

DOI: 10.1103/PhysRevE.76.050403 PACS number(s): 82.70.Dd, 61.20.Gy, 61.20.Ja

Colloidal systems consist of Brownian particles in a solvent [1]. They can be viewed as experimental analogs of atomic systems, as they can form liquid, crystal, and glassy phases [2]. Interestingly, the characteristic time and length scales of colloidal particles are larger than those in atomic systems, allowing their observation using optical microscopy [3]. They are ubiquitous in nature, as many biological liquids are colloidal suspensions of some type, and have many practical applications, including paints [4], biocatalysis [5], water purification [6], and photonic crystals [7,8].

Colloids are often immersed in water and stabilized through repulsive electrostatic interactions due to the presence of charge on the particles' surface [1], which arises from the dissociation of chemical groups. A possible consequence of this charging is the migration of particles toward the confining boundaries in order to minimize the total electrostatic energy of the system, as predicted theoretically [9–12]. In the presence of this electrostatic adsorption, the density profile of the system is characterized by a well-defined particle monolayer on the walls followed by a liquid-like structure in the bulk. When the confining boundaries are neutral, this effect can be thought of as resulting in a spontaneous charging of the walls.

From a practical point of view, this adsorption could be beneficial when inducing, for example, colloid crystallization or promoting deposition on surfaces [13]. It could also be unwanted, if it is the origin, for instance, of sample waste. Recently, this effect has been proposed to explain the rich phase behavior exhibited by mixtures of charged nanoparticles and neutral silica beads [14]. Up to now, however, there has been no clear exploration of the dependence of the effect in terms of controllable experimental parameters, such as particle charge, electrolyte concentration, and particle volume fraction.

In this Rapid Communication, we use Monte Carlo simulations to establish a state diagram that distinguishes between absorbing and nonabsorbing states. We find that for large enough interaction strength, range, and particle volume fraction, the system is characterized by the occurrence of electrostatic adsorption; this is in agreement with our intuition, as the increase in any of these variables raises the electrostatic energy of the system. We quantitatively describe the structural transition boundary found in simulations with theoretical calculations based on integral equations. Finally, we briefly show that our results can be used to predict the relevance of this effect in experiments.

We simulate a colloidal suspension based on spherical particles with surface charge Q and diameter σ at a volume fraction ϕ_0 in presence of their counter-ions and some added electrolyte, under the fulfillment of the electroneutrality condition. The solvent is a continuum with a dielectric constant $\varepsilon\varepsilon_0$, and the system is confined to a rectangular box of dimensions $L\times L\times L_z$ (Fig. 1). We consider uncharged confining walls and thus assume a hard-core interaction between the particles and the wall. The particles, however, interact through a screened Yukawa potential of the Derjaguin-Landau-Verwey-Overbeek (DLVO) form [15]

$$\frac{u(r)}{k_bT} = K\frac{e^{-\kappa(r-\sigma)}}{r}, \tag{1}$$

where the ions are considered pointlike and only contribute to the screening of the interaction. In this expression, r is the interparticle distance and $\kappa=\sqrt{\frac{e^2}{k_bT\varepsilon\varepsilon_0}\Sigma_i n_i Z_i^2}$ is the inverse of

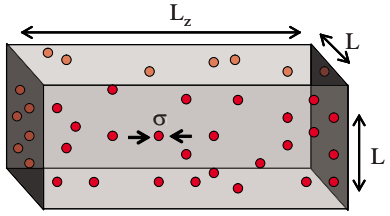

FIG. 1. (Color online) Schematic representation of the simulation box with the colloidal particles. The particle volume fraction ϕ_0 is adjusted by changing L.

*Present address: School of Physics, Georgia Institute of Technology, Atlanta, GA 30332.

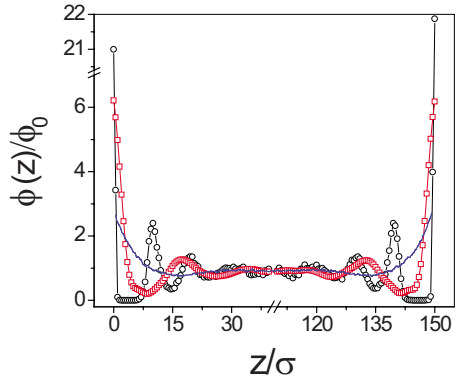

FIG. 2. (Color online) Equilibrium profiles in the normal direction to the confining walls, calculated from computer simulations. The volume fractions for the different curves are $\phi_0 \approx 3\times10^{-5}$ (blue solid line), $\phi_0 \approx 10^{-4}$ (red squares+line), and $\phi_0 \approx 5\times10^{-4}$ (circle+line). In all cases, $\kappa\sigma=0.15$ and $K=500\sigma$.

the Debye length, with n_i and Z_i the number concentration and the valence of the ith ionic species, e the electron charge, k_b the Boltzmann constant, and T the temperature. The strength of the interactions is given by $K=\frac{Q^2}{K_bT4\pi\varepsilon\varepsilon_0(1+\kappa\sigma/2)^2}$ and depends on both Q and κ. We neglect the attractive part of the DLVO potential as the typical distances we deal with are considerably larger than those at which the van der Waals attraction plays a relevant role [16].

Since we are interested in the equilibrium states of a system with a fixed number of particles, N, at constant T and inside a constant volume V, we perform Monte Carlo simulations in the canonical ensemble [18,19]. The average of magnitudes is obtained as integrals over all possible system configurations weighted with the canonical probability function $P=\frac{1}{Z_f}e^{-H(\vec{r}_1,\ldots,\vec{r}_N)/(k_bT)}$, where $H(\vec{r}_1,\ldots,\vec{r}_N)$ is the Hamiltonian of the system and Z_f is its partition function [20]. We employ a Metropolis algorithm to efficiently evaluate these averages [21]. The Monte Carlo sampling is generated by defining an initial configuration, choosing a random particle whose position is displaced from $\vec{r}_i$ to $\vec{r}_i+\delta\vec{r}_i$, evaluating the Hamiltonian change that results from such a displacement, $\Delta H=H(\vec{r}_1,\ldots,\vec{r}_i+\delta\vec{r}_i,\ldots,\vec{r}_N)-H(\vec{r}_1,\ldots,\vec{r}_N)$, and either accepting or rejecting the new configuration according to a probability factor $e^{-\Delta H/(k_bT)}$. We impose periodic boundary conditions in the directions x and y parallel to the walls, with $N=729$ particles. The particle volume fraction is changed by changing the dimension L of the simulation box. We allow the system to evolve toward equilibrium and obtain the density profiles in the direction z perpendicular to the walls by averaging the positions of the particles over 1000 equilibrium configurations.

Typical results are shown in Fig. 2, where we plot the local particle volume fraction $\phi(z)$ normalized with the initial volume fraction versus distance along the z direction for $K=500\sigma$, $\kappa\sigma=0.15$, and three values of ϕ_0. As can be seen, the three density profiles are symmetric with respect to $z=L_z/2$. We also note that the profiles in the central region of the cell are flat, with $\phi(z)=\phi_0$; this indicates that wall-particle correlations have already vanished at these wall-particle distances and that therefore the particles in this region behave as a bulk liquid. This feature also implies that the physics of the system would not change if only one wall is considered. For all initial volume fractions we have studied, the particle number close to the walls is larger than the particle number in the bulk; this is somehow equivalent to charging the walls. When this number of particles is large enough, a liquidlike structure is induced at larger distances. We define the occurrence of electrostatic adsorption when there is a nearest-neighbor peak with a height that exceeds the bulk value by 15% [22]. Thus, with this definition, electrostatic adsorption occurs when $\frac{\phi}{\phi_0}|_{nn}>1.15$. For $\phi_0\approx3\times10^{-5}$, the nearest-neighbor peak is almost absent, for $\phi_0\approx10^{-4}$ is right above the establish threshold, while at $\phi_0\approx5\times10^{-4}$, there is even an exclusion zone close to the walls that results from the large electrostatically induced charging of the plates [12].

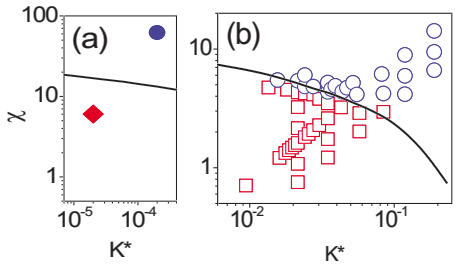

FIG. 3. (Color online) State diagram for electrostatic adsorption. (a) Theoretical predictions and results for two independent experiments (see text): ● $\sigma=1$ μm, $Q_{eff}\approx8\times10^3e$, $\phi_0\approx10^{-3}$, and $\kappa\sigma=6$. ◆ $\sigma=200$ nm, $Q_{eff}\approx5\times10^3e$, $\phi_0\approx10^{-2}$, and $\kappa\sigma=2.5$. (b) Theoretical predictions and simulation results: ○, no electrostatic adsorption; □, electrostatic adsorption.

By using this criterion we generate a state diagram for the occurrence of electrostatic adsorption, as shown in Fig. 3(b). The relevant variables of the system—namely, the strength and range of the electrostatic interactions and the initial particle volume fraction, which is related to the mean interparticle distance, $\bar{r}=\sigma\left(\frac{\pi}{6}\right)^{1/3}\phi_0^{-1/3}$—are encompassed in the two parameters $K^*=\frac{\bar{r}}{K}$ and $\chi=\kappa(\bar{r}-\sigma)$; we emphasize that these parameters completely characterize the state of the system, provided the only relevant interaction is the electrostatic repulsion between particles [23]. As can be observed, low values of χ or K^* revert in electrostatic adsorption. This is consistent with our intuition, as increasing the strength and range of the interaction and decreasing the mean particle distance raises the electrostatic energy of the system.

To theoretically account for this structural transition, we use the Ornstein-Zernike equation. Since there are wall-particle (w-p) and particle-particle (p-p) correlations in our system, there is an Ornstein-Zernike equation for each of these [25–28]:

$$h_{wp}(z)=c_{wp}(z)+2\pi\frac{N}{V}\int_0^{L_z}dz'h_{wp}(z')\int_{z-z'}^{\infty}ds\,sc_{pp}(s),$$

$$h_{pp}(r)=c_{pp}(r)+4\pi\frac{N}{V}\int_V c_{pp}(r)h_{pp}(r-r')r'^2dr', \quad (2)$$

where the total w-p and p-p correlations, which are described by the total correlation function $h(r)$, are decomposed into

direct and indirect contributions; these are given by the direct correlation function $c(r)$ and by the second term in Eq. (2) describing how the w-p and p-p correlations are mediated through the rest of the system. We note that $h(r)=g(r)-1$, where $g(r)$ is the pair correlation function that expresses the deviations of the system from ideal behavior.

In order to solve each of these equations, we need a closure relation for $c(r)$ and $h(r)$. We use the hypernetted chain equation (HNC) for the wall-particle correlation, which for the case of neutral walls reduces to [20]

$$c_{wp} = h_{wp}(z) - \ln[1 + h_{wp}(z)], \tag{3}$$

and a Rogers-Young (RY) closure for the particle-particle correlation; this is a more precise closure, as it is based on a mixture of the HNC and Percus-Yevick (PY) closure relations [29]:

$$1 + h_{pp}(r) = e^{-\beta u(r)}\left[1 + \frac{e^{\gamma(r)f(r)} - 1}{f(r)}\right], \tag{4}$$

where $\gamma(r)=h_{pp}(r)-c_{pp}(r)$ and $f(r)=1-e^{-\alpha r}$ is a mixing function bounded within 0 and 1. It is this last function that weights the relative proximity of this closure to the HNC and PY relations. The parameter α in $f(r)$ is chosen to achieve thermodynamic consistency [30].

These equations are solved numerically to obtain the transition between adsorbing and nonadsorbing states, as determined when the height of the first peak of $g(z)$ becomes 1.15 times its bulk value. The result is plotted in Fig. 3 in terms of the variables K^* and χ. There is excellent agreement with the simulations emphasizing the quality of the closure relations chosen. To further support our findings, we also present, in Fig. 3(a), the theoretical expectations together with two experimental cases of known absence and possible presence of electrostatic adsorption. In the first case [31], the experimental system consists of $\sigma \approx 1$ μm colloidal particles with effective charge $Q_{eff} \approx 8 \times 10^3 e$ at $\phi_0 \approx 10^{-3}$ and $\kappa = 6/\sigma$ (circle). Based on the position of the experimental point in the state diagram, no electrostatic adsorption is expected, in agreement with what was found experimentally. The other case is based on the observation of colloidal crystallization on the walls of dialysis tubing while eliminating ionic and unpolymerized rests after the synthesis of a colloidal suspension. Our observations pertain to microgel particles with $\sigma \approx 200$ nm, $Q_{eff} \approx 5 \times 10^3 e$, $\phi_0 \approx 10^{-2}$, and $\kappa = 2.5/\sigma$ [32]. The corresponding (K^*, χ) point (diamond) is located in the region where electrostatic adsorption is expected, which suggests that the observed wall crystallization occurs as a result of a purely electrostatically driven particle migration to the walls of the dialysis tubing; this is supported by the fact that no crystallization occurs until the conductivity of the water has decreased to approximately that of ultrapure water and thus until the range of the interaction has increased sufficiently.

In the experiment, the occurrence of electrostatic adsorption is reflected in the ordering within the confining walls. To verify that this is also the case in our simulations, we plot in Fig. 4 the two-dimensional pair correlation function $g(x,y)$ for representative adsorbing $[(K^*, \chi) = (0.02, 6.02)$, dashed line] and nonadsorbing $[(K^*, \chi) = (0.02, 1.61)$, solid line] states. As one might have anticipated, the establishment of a liquidlike structure in the bulk is accompanied by the establishment of a similar degree of order in the boundaries; this can be used in experiments to estimate the structure in the bulk, for instance, when the sample is observed with optical microscopy, but its opacity prevents the observation of the structure in the bulk.

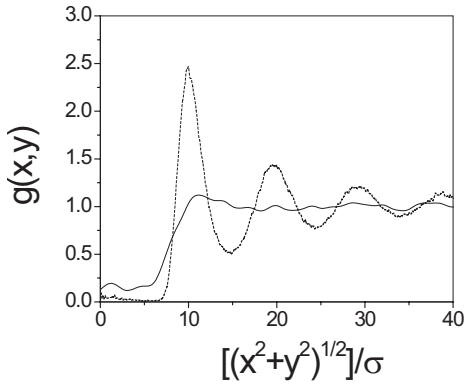

FIG. 4. Two-dimensional correlation function for the following points in the state diagram of Fig. 3: $K^* \approx 0.02$, $\chi \approx 1.61$ (dashed line); $K^* \approx 0.02$, $\chi \approx 6.02$ (solid line); these correspond to adsorbing and nonadsorbing states, respectively.

In conclusion, we have studied a model system of colloidal particles interacting through the repulsive part of a DLVO potential and confined between two neutral walls by means of Monte Carlo simulations. We have described the occurrence of electrostatic adsorption with a state diagram based on a pair of parameters, $\chi = \kappa(\bar{r} - \sigma)$ and $K^* = \frac{\bar{r}}{K}$, which include the relevant variables of the system. Our results are in quantitative agreement with theoretical calculations based on the integral Ornstein-Zernike equations. Furthermore, we have shown that these predictions capture some experimental observations, although such a comparison is only illustrative of the usefulness of our results; more extensive experimental comparisons are certainly needed. Additionally, we have verified that bulk structural properties are closely related with structural order in the surface of the confining walls, a fact that is also amenable to experimental check. Overall, our results can be used as a guide for experimentalists dealing with charged colloidal suspensions to estimate the relevance of electrostatic adsorption.

A.F-N. and J.J.L-S. acknowledge J.B. Caballero and A.M. Puertas for the computer support in the initial stages of this project and the support of Ministerio de Ciencia y Tecnologia (Grant No. MAT2004-03581). M.C-P. and M.M-N. acknowledge the support of the Consejo Nacional de Ciencia y Tecnología (CONACyT, Mexico) through Grant No. C01-47611.

[1] R. J. Hunter, *Foundation of Colloidal Science* (Clarendon Press, Oxford, 1989).
[2] V. J. Anderson and H. N. W. Lekkerkerker, Nature (London) **416**, 811 (2002).
[3] M. S. Elliot and W. C. K. Poon, Adv. Colloid Interface Sci. **92**, 133 (2001).
[4] S. Croll, Prog. Org. Coat. **44**, 131 (2002).
[5] F. Caruso, Adv. Mater. (Weinheim, Ger.) **13**, 11 (2001).
[6] M. Yoon *et al.*, J. Phys. Chem. B **105**, 2539 (2001).
[7] Y. N. Xia *et al.*, Adv. Mater. (Weinheim, Ger.) **12**, 693 (2000).
[8] A. Blanco *et al.*, Nature (London) **405**, 37 (2000).
[9] P. Gonzalez-Mozuelos and M. Medina-Noyola, J. Chem. Phys. **93**, 2109 (1990).
[10] P. Gonzalez-Mozuelos and M. Medina-Noyola, J. Chem. Phys. **94**, 1480 (1991).
[11] P. Gonzalez-Mozuelos, J. Alejandre, and M. Medina-Noyola, J. Chem. Phys. **95**, 8337 (1991).
[12] P. Gonzalez-Mozuelos, J. Alejandre, and M. Medina-Noyola, J. Chem. Phys. **97**, 8712 (1992).
[13] M. Giersig and P. Mulvaney, Langmuir **9**, 3408 (1993).
[14] V. Tohver *et al.*, Proc. Natl. Acad. Sci. U.S.A. **98**, 8950 (2001); S. Karanikas and A. A. Louis, Phys. Rev. Lett. **93**, 248303 (2004). The idea here is that electrostatic adsorption of nanoparticles onto neutral silica beads effectively charges the latter, giving rise to an unexpected system stabilization at high nanoparticle concentrations.
[15] B. V. Derjaguin and L. Landau, Acta Physicochim. URSS **14**, 633 (1941); E. J. Verwey and J. T. G. Overbeek, *Theory of the Stability of Lyophobic Colloids* (Elsevier, Amsterdam, 1948).
[16] In addition, we implicitly neglect that very close to the confining walls the interaction between particles can exhibit deviations from the DLVO potential, since the spherical symmetry of the colloid double layer could be broken [17]. A further improvement of our simplified model should take into account the counter-ions and salt ions as additional fluid species; this "primitive model" level of description goes beyond the Debye-Huckel screening mechanism that we adopt, which takes into account the small ions only through a space-independent screening parameter κ. The careful and systematic description of these complex effects, however, remains to be developed. Here we consider the simplest description of electrostatic adsorption phenomena, with the expectation that the global picture it provides will not be altered qualitatively by these effects.
[17] M. Medina-Noyola and B. I. Ivlev, Phys. Rev. E **52**, 6281 (1995); D. Goulding and J. P. Hansen, Mol. Phys. **95**, 649 (1998).
[18] B. Smit and D. Frenkel, *Understanding Molecular Simulation* (Academic Press, New York, 1996).
[19] M. P. Allen and D. J. Tildesley, *Computer Simulation of Liquids* (Clarendon, Oxford, 1987).
[20] D. A. McQuarrie, *Statistical Mechanics* (Harper & Row, New York, 1973).
[21] N. Metropolis *et al.*, J. Chem. Phys. **21**, 1087 (1953). By using this algorithm, we assume that the probability function P only depends on the previous configuration of the system.
[22] Taking this value equal to 10% or 20% does not significantly change the results, which are thus independent of the chosen criterion for electrostatic adsorption to occur. The particular selection simply reflects the relevant features of electrostatic adsorption: Accumulation of particles near the confining walls and establishment of liquidlike order in the bulk of the sample.
[23] We note that the Gillan's condition is fulfilled in our simulations [24]. Thus, the hard-core repulsion between particles is unimportant and the only relevant particle-particle interaction is of electrostatic nature.
[24] M. J. Gillan, J. Phys. C **7**, L1 (1974). See also G. Nagele, M. Medina-Noyola, R. Klein, and J. L. Arauz-Lara, Physica A **149**, 123 (1988).
[25] J.-P. Hansen and I. R. McDonald, *Theory of Simple Liquids* (Academic Press, New York, 1986).
[26] P. Hohenberg and W. Kohn, Phys. Rev. **136**, B864 (1964).
[27] R. Evans, Adv. Phys. **28**, 143 (1979).
[28] M. D. Mermin, Phys. Rev. **137**, A1441 (1965).
[29] F. J. Rogers and D. A. Young, Phys. Rev. A **30**, 999 (1984).
[30] The value of α is selected by equating the osmotic pressure calculated from a virial expansion and the osmotic pressure that is obtained from the osmotic compressibility to warranty that both are equal.
[31] J. J. Lietor-Santos, A. Fernandez-Nieves, and M. Marquez, Phys. Rev. E **74**, 051404 (2006).
[32] A. Fernandez-Nieves, A. Fernandez-Barbero, F. J. de las Nieves, Phys. Rev. E **63**, 041404 (2001); A. Fernandez-Nieves *et al.*, Macromolecules **33**, 2114 (2000).